Supplementary Information of

Constraining urban biogenic CO_2 fluxes: Composition, seasonality and drivers from radiocarbon and inventory analysis

Pingyang Li[1,2], Boji Lin[1,2,3], Zhihua Zhou[4,5,*], Jing Li[1,2], Zhineng Cheng[1,2], Jun Li[1,2], Sanyuan Zhu[1,2], Shizhen Zhao[1,2], Guangcai Zhong[1,2], Gan Zhang[1,2,*]

[1] State Key Laboratory of Advanced Environmental Technology, Guangzhou Institute of Geochemistry, Chinese Academy of Sciences, Guangzhou 510640, People's Republic of China

[2] Guangdong Key Laboratory of Environmental Protection and Resources Utilization, and Joint Laboratory of the Guangdong-Hong Kong-Macao Greater Bay Area for the Environment, Guangzhou Institute of Geochemistry, Chinese Academy of Sciences, Guangzhou 510640, People's Republic of China

[3] University of Chinese Academy of Sciences, Beijing 100049, People's Republic of China

[4] Shenzhen Ecological and Environmental Monitoring Center of Guangdong Province, Shenzhen 518049, People's Republic of China

[5] Guangdong Greater Bay Area, Change and Comprehensive Treatment of Regional Ecology and Environment, National Observation and Research Station, Shenzhen 518049, People's Republic of China

[*] Correspondence to: Gan Zhang (zhanggan@gig.ac.cn), Zhihua Zhou (zhou@zhihua.org)

Summary: 6 tables and 4 figures.

Table of Contents

Table S1. Comparison of CO_{2ff} and CO_{2bio} concentrations among cities

City	Time	Background	CO_{2ff} (ppm)	CO_{2bio} (ppm)	References
Paris	2010.02	MHD [a]	16.2 to 32.8	4.5 to 10.2	(Lopez et al., 2013)
Los Angeles	spring of 2010	LJO [b]	–	0.1 (min)	(Newman et al., 2016)
Los Angeles	winter 2012–2013	LJO	–	7.0 (max)	(Newman et al., 2016)
Los Angeles	2006-2013 winter	LJO	18.9 ± 1.2	4.1 ± 0.5	(Newman et al., 2016)
Los Angeles	2006-2013 summer	LJO	26.8 ± 0.4	2.2 ± 0.3	(Newman et al., 2016)
Los Angeles	2014.11 – 2016.03	MWO [c]	13.2 ± 9.4	1.5 ± 1.9	(Miller et al., 2020)
Los Angeles	2015.11-02	MWO	14.0 ± 12.7	3.5 ± 0.9	(Miller et al., 2020)
Los Angeles	2015. 05-09	MWO	13.2 ± 6.9	−0.3 ± 1.0	(Miller et al., 2020)
London	2020.05-07	MHD	12 to 20	−17 to −3	(Zazzeri et al., 2023)
Xi’an	2013.07	QXL [d]	–	−11.3 ± 10.0	(Zhou et al., 2020)
Xi’an	2015.10	QXL	–	51.6 ± 35.6	(Zhou et al., 2020)
Shenzhen	2022.04 – 2023.04	NL [e]	7.7 ± 3.7	–1.8 ± 4.1	This study

[a] Mace Head, [b] La Jolla, [c] Mount Wilson Observatory, [d] Qixianling, [e] Nanling

Table S2. CO_2 emissions from human respiration and excretion in Shenzhen

Age range (years old)	Body weight [a] (kg)		Respiratory emission rate [a] (g C d^{-1} $person^{-1}$)		Excretory emission rate [b] (g C d^{-1} $person^{-1}$)		Population [c] (million)		Respiratory emission (t C d^{-1})		Excretory emission (t C d^{-1})		Total emission (t C d^{-1})	
	Male	Female	Male	Female	Male	Female	Male	Female	Male	Female	Male	Female	Male	Female
0-4	13.80	12.80	109.73	96.80	25.23	23.41	0.53	0.47	58.43	45.19	13.44	10.93	71.87	56.11
5-9	27.20	25.50	155.65	135.85	49.74	46.63	0.52	0.44	81.47	60.02	26.03	20.60	107.50	80.62
10-14	44.20	42.60	199.78	170.88	80.82	77.90	0.39	0.32	77.54	54.02	31.37	24.63	108.91	78.64
15-19	63.90	55.00	248.13	193.34	116.85	100.57	0.39	0.27	95.84	51.46	45.13	26.77	140.97	78.24
20-24	73.80	54.96	341.20	237.40	134.95	100.50	0.96	0.75	327.22	178.09	129.42	75.39	456.65	253.47
25-29	73.80	54.96	371.32	256.52	134.95	100.50	1.39	1.10	516.26	282.66	187.62	110.74	703.89	393.40
30-34	73.98	58.14	358.19	267.28	135.28	106.31	1.52	1.16	543.24	310.53	205.17	123.51	748.41	434.04
35-39	73.98	58.14	361.12	274.10	135.28	106.31	1.12	0.88	405.58	241.95	151.93	93.84	557.51	335.79
40-44	72.38	61.18	359.59	284.52	132.35	111.87	0.80	0.63	286.02	179.81	105.27	70.70	391.29	250.51
45-49	72.38	61.18	359.51	282.54	132.35	111.87	0.73	0.61	262.87	171.37	96.77	67.85	359.64	239.22
50-54	72.24	63.62	356.28	277.11	132.10	116.33	0.57	0.48	204.22	133.38	75.72	55.99	279.94	189.37
55-59	72.24	63.62	348.22	266.98	132.10	116.33	0.36	0.33	124.35	88.66	47.17	38.63	171.52	127.30
60-64	71.46	63.32	278.26	238.06	130.67	115.79	0.18	0.20	50.39	46.80	23.66	22.76	74.05	69.57
65-69	71.46	63.32	268.97	235.70	130.67	115.79	0.13	0.15	35.42	35.35	17.21	17.37	52.63	52.72
70-74	68.36	59.50	252.54	217.47	125.00	108.80	0.07	0.07	16.60	15.26	8.21	7.64	24.81	22.90
75-79	68.36	59.50	241.25	209.73	125.00	108.80	0.03	0.04	7.65	8.10	3.96	4.20	11.61	12.30
>80	68.36	59.50	228.73	195.93	125.00	108.80	0.03	0.05	7.91	9.01	4.32	5.01	12.23	14.02
Total							9.72	7.94	3101.00	1911.65	1172.42	776.56	4273.42	2688.21
Total							17.66		5012.65		1948.98		6961.63	
Total (Mt CO_2 yr^{-1})		**2022**					17.66		**6.71**		**2.61**		**9.32**	
Total (Mt CO_2 yr^{-1})		**2023**					17.79		**6.76**		**2.63**		**9.38**	

[a] from Wang et al. (2024), [b] calculated referred to an average human mass of 70 kg with excretory emission rate of 128 g C d^{-1} $person^{-1}$ (Miller et al., 2020; Prairie and Duarte, 2007), [c] permanent resident population data for Shenzhen (2022 and 2023) from Shenzhen Statistical Yearbook 2023 and 2024 (Smbs, 2024, 2025). Age-sex group distributions using 2020 proportions obtained from Shenzhen Census Yearbook 2020 (Smbs, 2023).

Table S3. CO_2 emissions from livestock respiration in Shenzhen

Livestock species	Respiratory emission rate [a] (g C d^{-1} $head^{-1}$)	Production [b] (10^3 head)		Respiratory emission (kt CO_2 yr^{-1})	
		2022	2023	2022	2023
Horses	835.73	–	–	–	–
Pigs	53.04	118.3	60.2	**4.20**	**2.14**
Cattel and buffalo	594.52	1.387	1.41	**1.10**	**1.12**
Goats	87.95	–	–	–	–
Sheep	131.15	–	–	–	–
Chickens and ducks	3.42	1751.6	1172.7	**0.92**	**0.62**
Total				**6.22**	**3.88**

[a] derived from Elgar and Harvey (1987) and Freeman (1963), [b] data in 2022 and 2023 obtained from Shenzhen Statistical Yearbook 2023 and 2024, respectively (Smbs, 2024, 2025). We assumed that the life span of poultry, pigs, and other species is 42 days, half a year, and more than a year, respectively.

Table S4. Biogenic: fossil CO_2 emissions and ratios for human and livestock metabolism (HLM) and biomass burning (BB)

		SSY [a]	GRACED [b]	**R_{HLM}**	EDGAR2024 [c]	GRACED	**R_{BB}**	**R_{bio}**
Year	Month	HLM (Gg yr^{-1})	Fossil (Gg yr^{-1})	HLM: fossil	BB (Gg yr^{-1})	Fossil (Gg yr^{-1})	BB: fossil	Bio: fossil
2022		9326.2	55004.9	0.170	5046.1	55004.9	0.092	0.262
2023		9383.9	52849.3	0.178	4925.4	52849.3	0.093	0.271
April 2022 – April 2023		10111.7	58794.5	**0.178 ± 0.031**	5398.5	58794.5	**0.092 ± 0.015**	**0.270 ± 0.035**
2022	April	766.5	3518.7	0.218	371.7	3518.7	0.106	0.323
	May	792.1	4262.7	0.186	328.1	4262.7	0.077	0.263
	June	766.5	3292.3	0.233	304.9	3292.3	0.093	0.325
	July	792.1	3869.5	0.205	318.3	3869.5	0.082	0.287
	August	792.1	4857.1	0.163	335.5	4857.1	0.069	0.232
	September	766.5	4345.1	0.176	333.1	4345.1	0.077	0.253
	October	792.1	4899.9	0.162	408.8	4899.9	0.083	0.245
	November	766.5	4370.6	0.175	489.0	4370.6	0.112	0.287
	December	792.1	5844.2	0.136	621.4	5844.2	0.106	0.242
2023	January	797.0	797.0	0.119	563.0	6692.7	0.084	0.203
	February	719.9	719.9	0.159	519.0	4526.3	0.115	0.274
	March	797.0	797.0	0.189	444.2	4218.5	0.105	0.294
	April	771.3	771.3	0.188	361.4	4096.9	0.088	0.276

[a] SSY is the Shenzhen Statistical Yearbook with data from results in Tables S2 and S3. [b] GRACED is the near-real-time Global Gridded Daily CO_2 Emissions Dataset.

[c] EDGAR is the Emissions Database for Global Atmospheric Research; we assume that CO_{2BB} emissions account for 100 % of CO_{2bio} in EDGAR2024.

Table S5. Comparison of contributions to urban CO_{2bio} from different cities

City	Time	Inventory	Human respiration and excretion (%)	Biofuel use or biomass burning (%)	Net plant and soil respiration or terrestrial biosphere (%)		References
					Belowground respiration	Aboveground respiration	
Los Angeles	2007.10	–	–	–	38	62	(Djuricin et al., 2010)
Los Angeles	2007.12	–	–	–	46	54	(Djuricin et al., 2010)
Los Angeles	2008.02	–	–	–	22	78	(Djuricin et al., 2010)
Los Angeles	2008.04	–	–	–	15	85	(Djuricin et al., 2010)
Paris	2010.01–02	AirParif (2008.01)	50 [a] / 15.0 [a, d]	12 [b] / 1.2 [b, d]	38 [c] / 83.8 [c, d]		(Lopez et al., 2013)
Los Angeles	2014.11–2016.03	Hestia–L.A. (2012)	5.7 [d]	10.3 [d]	84.0 [d]		(Miller et al., 2020)
Beijing	2020 winter	GRACED (2020)	7.5 [a, d]	–	–		(Wang et al., 2024)
Shenzhen	2022.04–2023.04	GRACED (2022–2023)	17.8 ± 3.1 [d, e]	9.2 ± 1.5 [d]	73.0 ± 3.5 [d]		This study
Shenzhen	2022	GRACED (2022)	17.0 [d, e]	9.2 [d]	73.8 [d]		This study
Shenzhen	2022	ODIAC2022 (2021)	10.5 [d, e]	5.7 [d]	83.8 [d]		This study
Shenzhen	2022	MIXv2 (2017)	13.9 [d, e]	7.5 [d]	78.6 [d]		This study
Shenzhen	2022	EDGARv7.0 (2021)	16.4 [d, e]	8.9 [d]	74.7 [d]		This study
Shenzhen	2022	MEICv1.4 (2020)	20.9 [d, e]	11.3 [d]	67.8 [d]		This study

[a] only human respiration, [b] use of biofuel in gasoline and diesel, [c] soil respiration, [d] ratio to fossil fluxes, [e] human and livestock metabolism

Table S6. Comparison of climatic characteristic and CO_{2bio}' in representative cities across two typical climate zones

Climate zone	**Mediterranean climate**	**Monsoon influenced humid subtropical climate**
Representative city	Los Angeles	Shenzhen
Population (million)	~18	~18
Area (km^2)	15,000	~2,000
Location (latitude and longitude)	Lower mid-latitudes (34.13°N, −118.13°E)	Low latitudes (22.54°N, 114.06°E)
Climate characteristics	Hot and dry summers Mild and wet winters	Hot and wet summers Cool and dry winters
MODIS VCF [a] (%)	14%	73%
Land cover (fraction)	Built area and water (61%) [b] **Tree (21%)** **Irrigated lawn (12%)** Dry grass/bare soil (6%)	Built area and water (42.7%) [c] **Tree (55.6%)** Grass (0.6%) Bare soil (1.1%)
Monthly mean CO_{2bio}' minima	−3.5 ppm in July	−12.8 ppm in September
CO_{2bio}' seasonal amplitude	4.3 ppm	11.5 ppm
Driver factor of CO_{2bio}' seasonal variation	**Irrigation water usage**	**Atmospheric temperature**
Reference	Miller et al. (2020)	This study

[a] VCF represents Vegetation Continuous Fields, [b] derived from Mcpherson et al. (2011), [c] obtained from Qian et al. (2020).

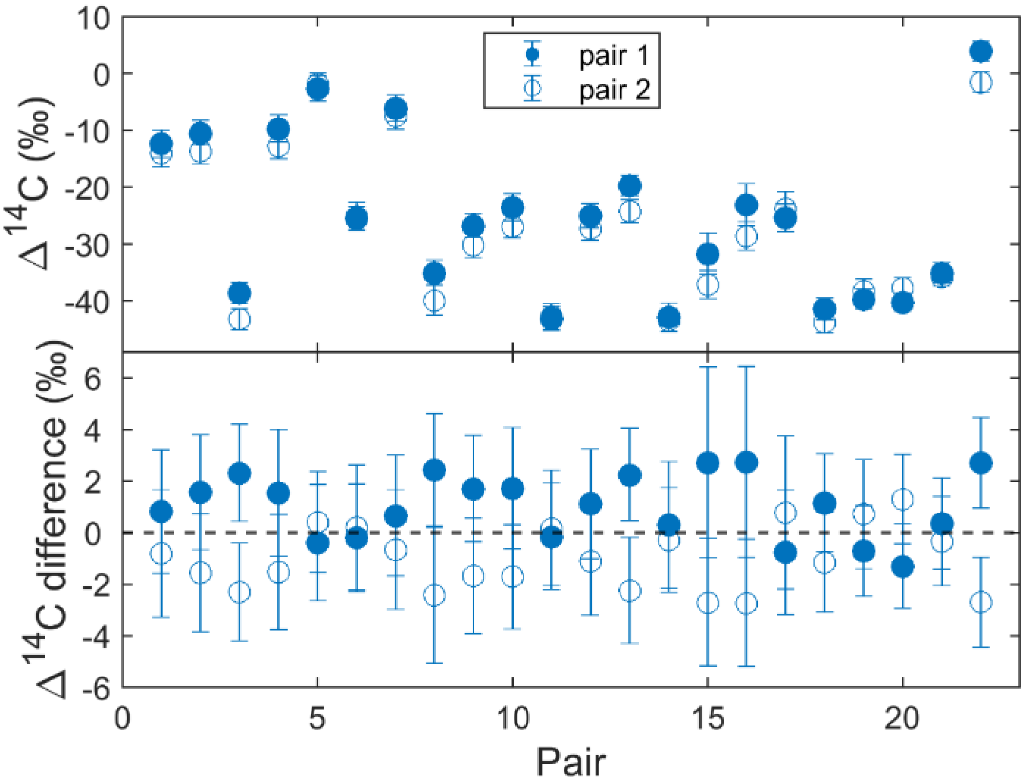

Figure S1. Pair differences of $\Delta^{14}C$ for replicate measurements

Replicates were obtained from parallel air samples. The difference of each individual measurement from its pair mean is shown. Closed and open symbols are the first and second group taken from each pair, respectively. Error bars are the 1-sigma uncertainty on each measurement.

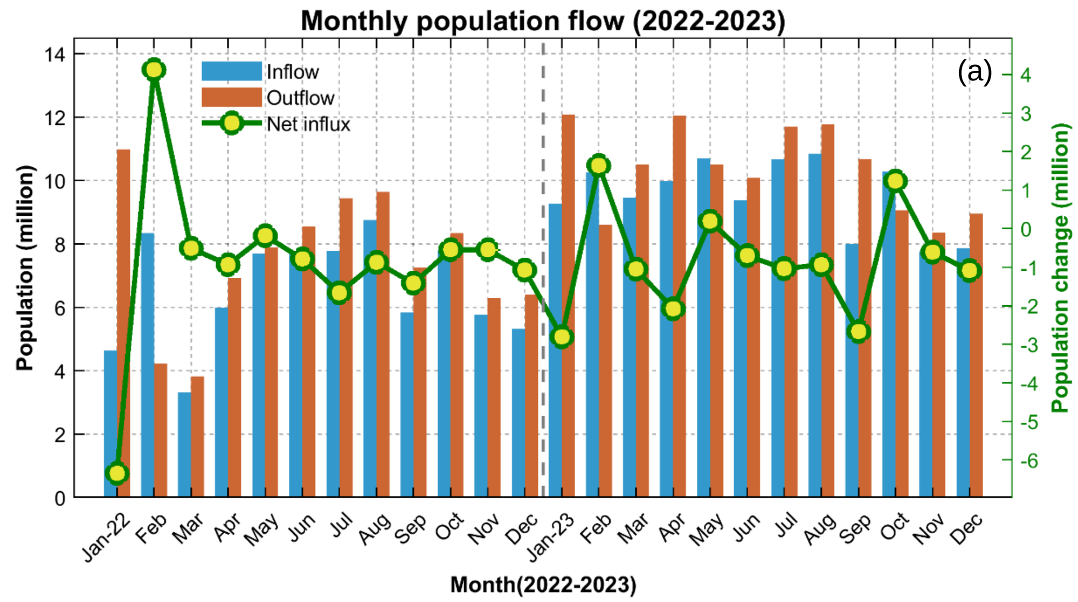
Monthly population flow (2022-2023)
(a)
Inflow
Outflow
Net influx
Population (million)
Population change (million)
Jan-22 Feb Mar Apr May Jun Jul Aug Sep Oct Nov Dec Jan-23 Feb Mar Apr May Jun Jul Aug Sep Oct Nov Dec
Month(2022-2023)

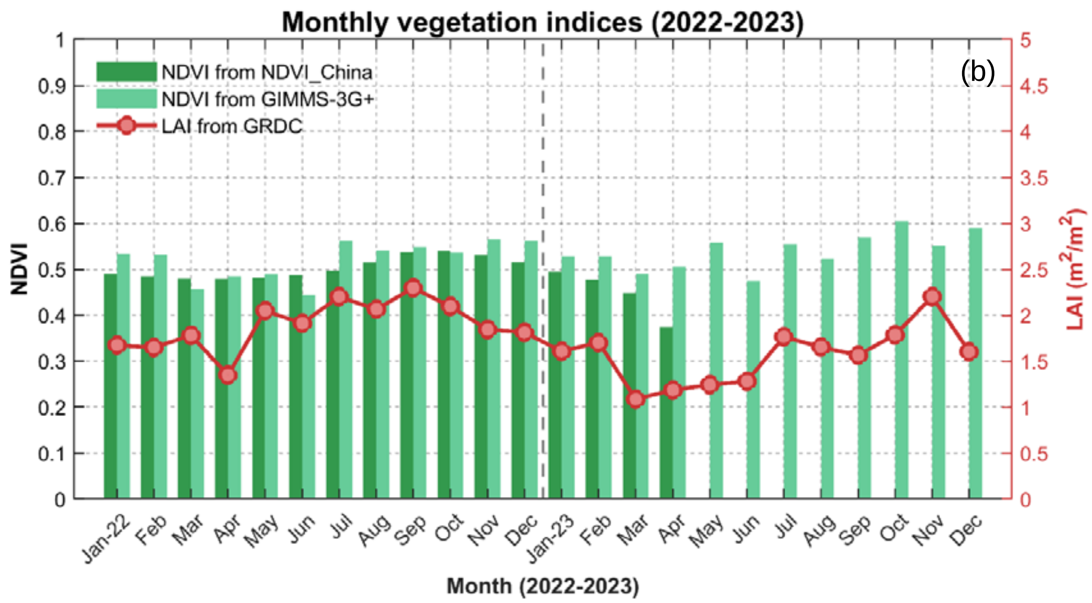
Monthly vegetation indices (2022-2023)
(b)
NDVI from NDVI_China
NDVI from GIMMS-3G+
LAI from GRDC
NDVI
LAI (m2/m2)
Jan-22 Feb Mar Apr May Jun Jul Aug Sep Oct Nov Dec Jan-23 Feb Mar Apr May Jun Jul Aug Sep Oct Nov Dec
Month (2022-2023)

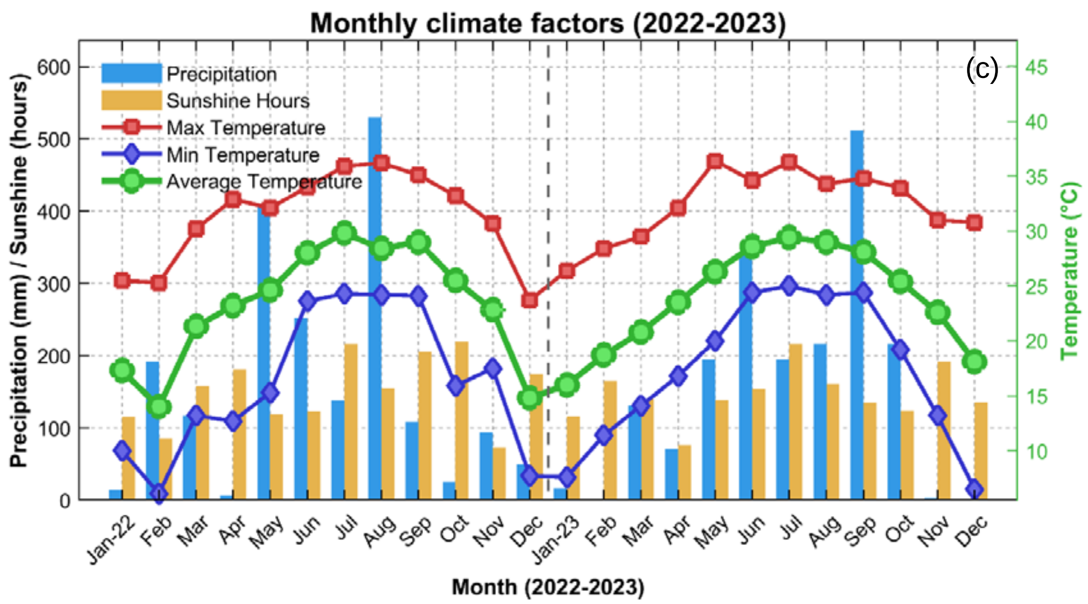
Monthly climate factors (2022-2023)
(c)
Precipitation
Sunshine Hours
Max Temperature
Min Temperature
Average Temperature
Precipitation (mm) / Sunshine (hours)
Temperature (°C)
Jan-22 Feb Mar Apr May Jun Jul Aug Sep Oct Nov Dec Jan-23 Feb Mar Apr May Jun Jul Aug Sep Oct Nov Dec
Month (2022-2023)

Figure S2. Monthly (a) population flow, (b) vegetation indices, and (c) climate factors in 2022 and 2023

Population flow includes population inflow, outflow, and net influx (inflow – outflow). Vegetation indices include NDVI from NDVI_China and GIMMS-3G+, and LAI from GRDC. Climate factors include temperature, precipitation, and sunshine hours.

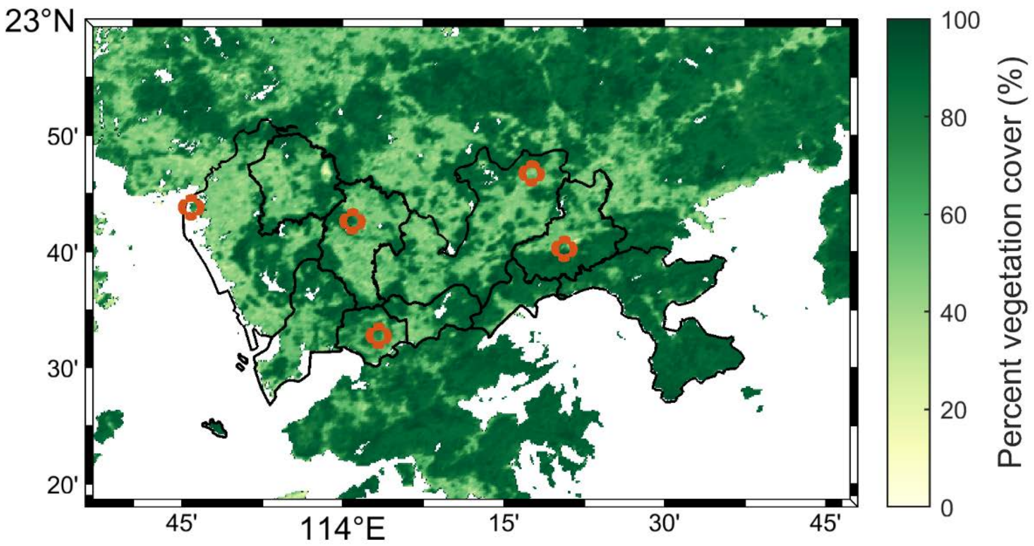

Figure S3. Percent vegetation cover in Shenzhen and its surrounding areas from MODIS Vegetation Continuous Fields

The red circles represent the "signal" sites in the study. The live vegetation fractions during March 6, 2022 – March 6, 2023 were derived from the Moderate Resolution Imaging Spectroradiometer (MODIS) Vegetation Continuous Fields (VCF, product MOD44Bv061) (Dimiceli, 2024), which provide a yearly continuous and quantitative representation of land surface cover at a spatial resolution of 250 m. The mean and standard deviation of the vegetation fraction is 73.3 ± 18.6% for the Shenzhen area. In order to calculate the mean vegetation fraction in the footprint of our measurements, we convolved the FLEXPART monthly footprints with the combined vegetation fraction map (both at 0.05° × 0.05°) for each air sample as $V_{frac} = \sum(VCF\_map \times \mathrm{F}ootprint)/\sum Footprint$. The means and standard deviations of the footprint-weighted vegetation fraction for the five sites are 72.0 ± 56.7%, 65.5 ± 52.5%, 74.6 ± 50.3%, 78.5 ± 55.7%, and 70.3 ± 48.4%, respectively.

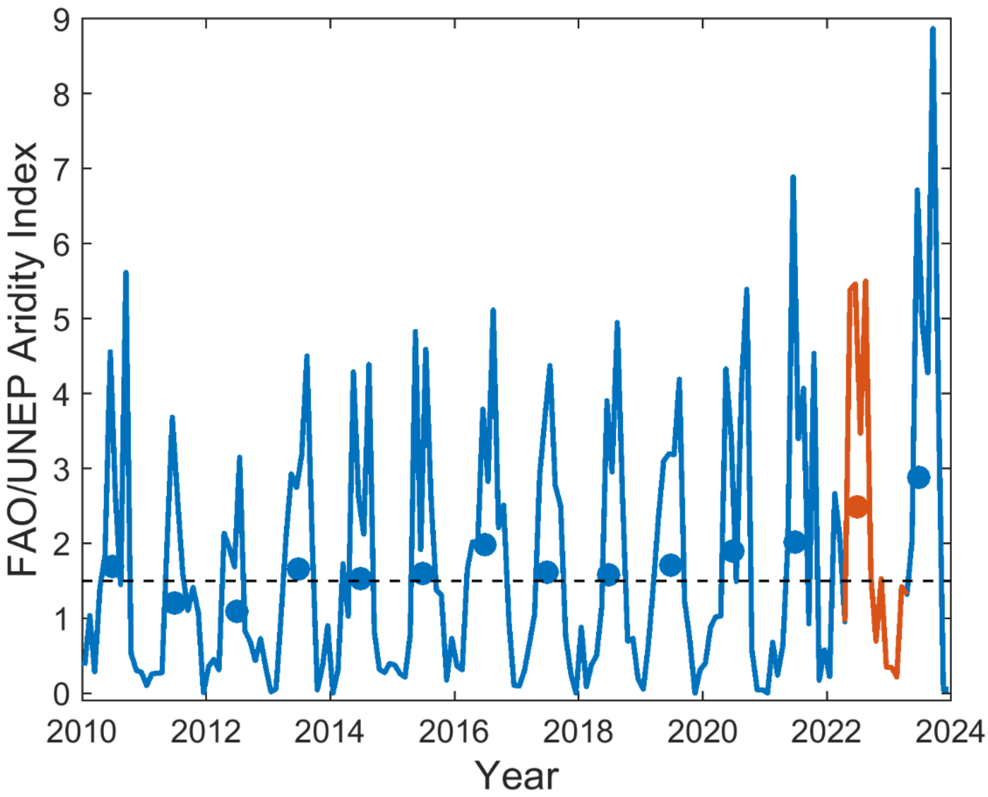

Figure S4. FAO/UNEP Aridity Index (AI) for Shenzhen area between 2010 and 2023

The Food and Agriculture Organization/ United Nations Environment Programme (FAO/UNEP) Aridity Index (AI), defined as the ratio of Mean Annual Precipitation (MAP in mm) to Potential Evapotranspiration (PET in mm), indicates water balance between land surface and atmosphere (Schlaepfer et al., 2017). MAP and PET data are derived from the Climatic Research Unit Time Series dataset (CRU TS4.08, http://badc.nerc.ac.uk/, last accessed on 24 September 2024) (Harris et al., 2020). The solid line shows monthly values and the filled circles show annual means. The period from April 2022 to April 2023 corresponding to the $\Delta^{14}C$ time series in this study is shown in red. According to the methodology from the FAO (Singh, 1993), four climate zones are classified: arid zone (AI < 0.5), semi-arid/ humid zone ($0.5 \leq AI < 1$), humid zone ($1 \leq AI < 1.5$), and extreme humid zone ($1.5 \leq AI$, the dashed line) (Liao et al., 2023). We found that Shenzhen is in the extreme humid zone from 2013 to 2023.

References

DiMiceli, C.: MOD44B MODIS/Terra Vegetation Continuous Fields Yearly L3 Global 250m SIN Grid V061 [Data set] [dataset], https://doi.org/10.5067/MODIS/MOD44B.061, 2024.

Djuricin, S., Pataki, D. E., and Xu, X.: A comparison of tracer methods for quantifying CO_2 sources in an urban region, J. Geophys. Res. Atmos., 115, D11303, https://doi.org/10.1029/2009JD012236, 2010.

Elgar, M. A. and Harvey, P. H.: Basal Metabolic Rates in Mammals: Allometry, Phylogeny and Ecology, J Functional Ecology, 1, 25-36, 1987.

Freeman, B. M.: Gaseous metabolism of the domestic chicken: IV. The effect of temperature on the resting metabolism of the fowl during the first month of life, J British Poultry Science, 4, 275-278, 1963.

Harris, I., Osborn, T. J., Jones, P., and Lister, D. J. S. d.: Version 4 of the CRU TS monthly high-resolution gridded multivariate climate dataset, 7, 109, 2020.

Liao, J., Dai, Y., An, L., Hang, J., Shi, Y., and Zeng, L.: Water-energy-vegetation nexus explain global geographical variation in surface urban heat island intensity, Sci. Total Environ., 895, 165158, https://doi.org/10.1016/j.scitotenv.2023.165158, 2023.

Lopez, M., Schmidt, M., Delmotte, M., Colomb, A., Gros, V., Janssen, C., Lehman, S. J., Mondelain, D., Perrussel, O., Ramonet, M., Xueref-Remy, I., and Bousquet, P.: CO, NO_x and $^{13}CO_2$ as tracers for fossil fuel CO_2: results from a pilot study in Paris during winter 2010, Atmos. Chem. Phys., 13, 7343–7358, 10.5194/acp-13-7343-2013, 2013.

McPherson, E. G., Simpson, J. R., Xiao, Q., and Wu, C.: Million trees Los Angeles canopy cover and benefit assessment, Landscape and Urban Planning, 99, 40-50, https://doi.org/10.1016/j.landurbplan.2010.08.011, 2011.

Miller, J. B., Lehman, S. J., Verhulst, K. R., Miller, C. E., Duren, R. M., Yadav, V., Newman, S., and Sloop, C. D.: Large and seasonally varying biospheric CO_2 fluxes in the Los Angeles megacity revealed by atmospheric radiocarbon, Proc. Natl. Acad. Sci., 117, 26681–26687, 2020.

Newman, S., Xu, X., Gurney, K. R., Hsu, Y. K., Li, K. F., Jiang, X., Keeling, R., Feng, S., O'Keefe, D., Patarasuk, R., Wong, K. W., Rao, P., Fischer, M. L., and Yung, Y. L.: Toward consistency between trends in bottom-up CO_2 emissions and top-down atmospheric measurements in the Los Angeles megacity, Atmos. Chem. Phys., 16, 3843–3863, 10.5194/acp-16-3843-2016, 2016.

Prairie, Y. T. and Duarte, C. M.: Direct and indirect metabolic CO_2 release by humanity, Biogeosciences, 4, 215-217, 10.5194/bg-4-215-2007, 2007.

Qian, Y., Zhou, W., Pickett, S. T. A., Yu, W., Xiong, D., Wang, W., and Jing, C.: Integrating structure and function: mapping the hierarchical spatial heterogeneity of urban landscapes, Ecol. Process., 9, 59, 10.1186/s13717-020-00266-1, 2020.

Schlaepfer, D. R., Bradford, J. B., Lauenroth, W. K., Munson, S. M., Tietjen, B., Hall, S. A., Wilson, S. D., Duniway, M. C., Jia, G., Pyke, D. A., Lkhagva, A., and Jamiyansharav, K.: Climate change reduces extent of temperate drylands and intensifies drought in deep soils, Nat. Commun., 8, 14196, 10.1038/ncomms14196, 2017.

Singh, K.: Forest resources assessment 1990: tropical countries, FAO Forestry Paper 112, United Nations Food and Agriculture Organization, Rome1993.

Shenzhen Census Yearbook 2020: https://tjj.sz.gov.cn/gkmlpt/content/10/10688/post_10688160.html#4219 (last access: 20 June 2024), last

(Shenzhen Municipal Bureau of Statistics), Shenzhen Statistical Yearbook 2023: https://tjj.sz.gov.cn/gkmlpt/content/11/11182/post_11182604.html#4219 (last accessed: 14 March 2024), last

(Shenzhen Municipal Bureau of Statistics), Shenzhen Statistical Yearbook 2024: https://tjj.sz.gov.cn/zwgk/zfxxgkml/tjsj/tjnj/content/post_12061198.html (last accessed: 25 May 2025), last

Wang, P., Zhou, W., Niu, Z., Huo, D., Zhou, J., Li, H., Cheng, P., Wu, S., Xiong, X., and Chen, N.: An Approach for Assessing Human Respiration CO2 Emissions Using Radiocarbon Measurements and Bottom-Up Data Sets, J. Geophys. Res. Atmos., 129, e2023JD040578, https://doi.org/10.1029/2023JD040578, 2024.

Zazzeri, G., Graven, H., Xu, X., Saboya, E., Blyth, L., Manning, A., Chawner, H., Wu, D., and Hammer, S.: Radiocarbon Measurements Reveal Underestimated Fossil CH_4 and CO_2 Emissions in London, Geophys. Res. Lett., 50, e2023GL103834, 10.1029/2023GL103834, 2023.

Zhou, W. J., Niu, Z. C., Wu, S. G., Xiong, X., Hou, Y., Wang, P., Feng, T., Cheng, P., Du, H., and Lu, X.: Fossil fuel CO_2 traced by radiocarbon in fifteen Chinese cities, Sci. Total Environ., 729, 138639, 2020.